Computers and Electronics in Agriculture 143 (2017) 57–65

Contents lists available at ScienceDirect

Computers and Electronics in Agriculture

journal homepage: www.elsevier.com/locate/compag

Original papers

Simulation study of vibratory harvesting of Chinese winter jujube (*Zizyphus jujuba* Mill. cv. Dongzao)

Jun Peng[a], Hongqi Xie[a], Yali Feng[a], Longsheng Fu[a,b,c,*], Shipeng Sun[a], Yongjie Cui[a]

[a] College of Mechanical and Electronic Engineering, Northwest A & F University, Yangling 712100, China
[b] Key Laboratory of Agricultural Internet of Things, Ministry of Agriculture, Yangling 712100, China
[c] Center for Precision & Automated Agricultural Systems, Washington State University, Prosser, WA 99350, USA

ARTICLE INFO

Keywords:
Chinese winter jujube
Finite element analysis
Vibratory harvesting
Simulation
Acceleration distribution

ABSTRACT

Chinese winter jujube is rich in nutrition, but its harvesting is labor-intensive. A feasible method for mechanical harvesting of Chinese winter jujube is vibration harvesting. Currently, harvesting shakers for jujube were designed and optimized mainly based on imperial method through field experiments which are complex, time-consuming and limited by time and environment. In order to improve the rationality in shaker design, a better understanding of the interaction between the shaker and the tree is necessary. The aim of this study was to develop a simulation framework for predicting the responses of trees under vibration excitation with a shaker using finite element methods, and find relationships between the responses and the excitation frequencies. Field experiments were conducted using a shaker at five frequencies (5, 10, 15, 20, and 25 Hz) with three replicated trees. The input force was measured by a tension sensor and the acceleration of trees was measured by tri-axial acceleration transducers. The trees were modeled using Autodesk Inventor 2014 and then simulated by finite element method in ANSYS 15.0. In simulation, the tree model was divided to two parts, including branches and trunk. For both parts, the wood's mechanical properties were determined experimentally. Results show that the acceleration value of experiment is generally larger than that of simulation, and it increases from the bottom of branch to the top. The acceleration curves in both experimental and simulation conditions and the distribution nephograms indicated that the greater frequency of tree shaking generates greater acceleration. The mean correlation coefficients of acceleration between experiment and simulation is 0.62. The average resultant accelerations of measured and simulated showed a good alignment in changing trends. It can be concluded that the simulation is promising for studying the response of trees under the vibration excitation of the shaker.

1. Introduction

Chinese winter jujube (*Ziziphus jujuba* Mill.) is an indigenous tree to China and famous for its good taste and rich nutrition of fruit. Chinese jujube is one type of tree fruit crops belonging to Rhamnaceae group and has been cultivated since 4000 years ago. It is also a variety compatible with the present ecology and economy with the function of environmental reservation as an economic crop (Gao et al., 2011; Zhang et al., 2016). Chinese winter jujube is a kind of fresh jujube, which is deeply favored by people for its good taste and abundant nutrition, such as vitamin C, amino acids, cyclic AMP, carbohydrate, and minerals (Li et al., 2007; Sun et al., 2007). The jujube fruit are also used as some medicinal supplements, such as tonic medicine and health supplement for blood nourishment and sedation (Gao et al., 2013; Lam et al., 2016; Plastina et al., 2012).

Current methods in harvesting jujube fruits are labor intensive and time consuming, which needs develop an efficient and economical harvesting technologies to keep jujube industry sustainability. Previous researches showed that vibrating or shaking is one of the feasible methods of mechanical harvesting for jujube. Lee et al. (2003) developed a canopy jujube shaker which achieved a detachment rate of 95.8% at 6.7 Hz with 5 s. However, the high intensity of shaking impact of the shaker resulted in a high rate of fruit damage of 10.7%, most of which was caused by the direct contact between jujube fruits and the harvester during fruit separation. A jujube trunk shaking harvester prototype was developed by the Xinjiang Academy of Agricultural and Reclamation Science. The harvester is able to run at 9.0 or 16.7 Hz, and harvest 76 trees per hour with a detachment rate of 90% and fruit damaged less than 0.2% (Meng et al., 2013). Fu et al. (2014) designed a self-propelled canopy shaker for jujube, which works riding on trees and shakes branches to induce inertial force on the fruits by rods mounted on the shaker. The shaker was reported that it removed 96.2%

* Corresponding author.
E-mail addresses: fulsh@nwafu.edu.cn, longsheng.fu@wsu.edu (L. Fu).

http://dx.doi.org/10.1016/j.compag.2017.09.036
Received 22 August 2016; Received in revised form 22 August 2017; Accepted 25 September 2017
Available online 16 October 2017
0168-1699/

fruit from trees when it was operated at a traveling speed of 0.3 m/s, amplitude of 9 mm, frequency of 15 Hz, and vibration duration of 17 s, while fruit and branches damage were reported as less than 2.8%. Although those shakers were significantly improved the harvesting efficiency, the development was dependent on imperial design and needs theoretical studies to identify relationships between jujube trees and vibration frequency.

Researchers have conducted field experiments to study the tree-shaker system, fruit-stem subsystems or tree systems using different types of shaker to harvest fruits. Savary et al. (2011) investigated the force and acceleration distribution on citrus tree branches and fruits. Du et al. (2012) studied sweet cherry tree acceleration responses under sinusoidal excitations, and quantified the distribution and dissipation of applied vibratory energy within the woody structure of cherry trees. Zhou et al. (2013) conducted a field experiment for identification of the suitable shaking frequency and duration in mechanical harvesting of sweet cherry. Wu et al. (2014) reconstructed a three-dimensional (3D) Chinese hickory tree and performed a dynamics analysis for the reconstructed tree using field experiment. However, these field experiment methods are complex, time-consuming and also limited by time and environment.

Another approach for optimizing shaker design is using finite element method to simulate fruit harvesting. Yung and Fridley (1975) developed a finite element model for an apple tree system. Upadhyaya et al. (1981) established a finite element model for the dynamics of branch based on linearized beam theory. Láng (2008) calculated the relationship between power consumption and trunk amplitude for all trunk cross-sections, and found the most efficient clamping heights of the shakers. Savary et al. (2010) simulated citrus tree canopy motion during harvesting using a canopy shaker. Tang et al. (2011) researched the vibration characteristics of wolfberry tree using the finite element method. Bentaher et al. (2013) studied the optimization of stem shaking conditions in the mechanical harvesting of olive fruits and the influence of different shakers on the dynamic response of olive tree by finite element analysis. Tinoco et al. (2014) used the finite element method to analyze mechanical properties of the fruit-peduncle of coffee. Fu et al. (2016) applied modal analysis and harmonic response analysis to determine the natural frequency and steady-state response of sea buckthorn tree to study the tree responses to shaking frequency and amplitude. In these studies, several assumptions were made to create the simulation models such as, ignoring the existence of leaves and fruits and assuming unified mechanical properties of the trunk and all branches. Although, these assumptions would cause differences between simulation results and pertinent practical application, they have been good indicators of how harvesting in reality might be.

In practice, branches of Chinese winter jujube are pruned every year to maintenance dwarf tree size, which makes differences in the mechanical properties between the trunk and branches. To our knowledge, there is no previous research considered this variation. In order to improve the simulation results toward further resembling of actual harvesting situation, the goal of this study was to develop simulation framework for evaluation of tree response to shaking excitation. The specific objectives included (1) measurement of the mechanical properties of the trunk and branches separately, (2) study of the acceleration and frequency response of jujube tree, and (3) establishment of 3D finite element models of jujube trees to develop and evaluate simulation framework. It aimed for studying the acceleration during vibration to predict the responses of trees under the vibration loading and find the relationship between the responses and frequencies of excitation.

2. Materials and methods

2.1. Mechanical properties measurement

This study was conducted in a private fruit orchard (34°89′31″N, 109°92′53″E, and 366 m in altitude) at Xuzhuang Town, Dali County, Shaanxi Province, China. Three 6-year-old winter jujube trees (Tree 1, Tree 2, and Tree 3) were randomly selected from the orchard. The material properties of the trees were determined from fresh wood samples of trunk and branch which were selected randomly from the trees after the field experiment. Fig. 1 shows the different samples used for this experiment.

Fig. 1. Wood samples for measuring mechanical properties of trunk and branch.

The moisture of the trunk and branches were measured using a digital moisture meter (TESTO 606-1, Testo SE & Co., Lenzkirch, Germany) with a sensitivity of 0.1%. The density was measured by the water displacement method at 20 °C (Razavi and BahramParvar, 2007). The density ρ (kg/m^3) of wood samples was calculated by the following equation.

$$\rho = \frac{M_a}{M_a - M_w}\rho_w \tag{1}$$

where M_a is the mass of a sample in air (kg), M_w is the mass of the sample in water (kg), and ρ_w is the density of water (kg/m^3). The density of water was conducted by an electronic density meter (DH-600, Dongguan Hongtuo Instrument Co., Ltd., Guangdong, China) with a sensitivity of 1.0 kg/m^3.

The elastic modulus of wood was determined experimentally on a traction machine (DDL10, Changchun Research Institute for Mechanical Science Co., Ltd, Jilin, China) in grain direction (Krauss, 2007). The young's modulus E (Pa) can be obtained by Eq. (2).

$$E = \frac{\Delta F l}{\Delta l A} \tag{2}$$

where $\triangle F$ is the force increment (N), l is the length of the sample (m), $\triangle l$ is the length increment (m), and A is the cross-section dimension of sample (m^2).

Shear modulus is the slope of the stress-strain curve when a shearing force is applied to the samples. In this study, the shear modulus was determined by a torsion method (Stoffler, 1980). This method restrains a specimen from rotating at one end while imposing a twisting moment at the other end. The torque and angle were measured by a microcomputer-controlled torsion measurement device (NWS500, Changchun Research Institute for Mechanical Science Co., Ltd, Jilin, China). The shear modulus G (Pa) can be obtained by Eq. (3).

$$G = \frac{\Delta T L_0}{\Delta \phi I_p} \tag{3}$$

where $\triangle T$ is the torque increment (N m), L_0 is the gauge length of specimen (m), $\triangle \Phi$ is the angle increment (rad), and I_p is the polar moment of inertia of specimen (m^4).

The Poisson ratio μ (no unit) is calculated by Eq. (4):

$$\mu = \frac{(E-2G)}{2G} \tag{4}$$

where G is the shear modulus (Pa) and E is the Young's modulus (Pa).

When a damped system is struck by an impulsive load or is released from a displaced position relative to its equilibrium state, a decaying oscillation occurs. The energy of damping losses is expressed in terms of damping ratio. The damping ratio is inherent attributes of materials, which is a dimensionless measure describing how oscillations in a system decay after a disturbance (Jing and Lang, 2009). The default is that the damping ratio of trunk is the same as branches.

Damping ratio of branch was measured through a vibration test. Test samples were selected from main branches of the three experimental trees. The branch samples was 26 mm in average diameter and 300 mm in average length. A measurement of damping called logarithmic decrement δ is defined as the natural logarithm of the ratio of amplitudes of successive peaks (Jing and Lang, 2009). The impulsive load was generated by the impact hammer (LC-1, Far East Vibration System Engineering Technology Co., Ltd, Beijing, China), and the response was measured by acceleration transducer (DH311E, Donghua Testing Technology Co., Ltd, Taizhou, China).

$$\delta = \ln\frac{A_1}{A_2} = \frac{1}{N}\ln\frac{A_1}{A_{1+N}} \tag{5}$$

$$\zeta = \frac{\delta}{\sqrt{4\pi^2 + \delta^2}} \tag{6}$$

where δ is the logarithmic decrement (no unit), A_1, A_2, A_{1+N} are amplitudes of the first, second and (1 + N)th peak, respectively (m), ζ is the damping ratio (no unit).

2.2. Modeling the trees

The trees used in the simulation were modeled in Autodesk Inventor 2014 (Autodesk Inc., San Rafael, USA). The diameters at different locations along the branches were measured under the assumption that the branch section is circular. A local Cartesian coordinate system was assigned to each tree, and the coordinate and diameter of each point were measured based on this coordinate system in the field experiment. The diameter of tree branches was measured by vernier calipers. The measured points were plotted in 3D sketch, and a 3D spline was drawn connecting them in Autodesk Inventor 2014. At each point, a reference plane which is normal to the 3D spline was drawn. The circular cross section was drawn on these planes using the diameters measured. Using the cross sections as outline curve and spline as the guide curve, the tree was drawn using the sweep feature in Autodesk Inventor 2014. Fig. 2 showed the 3D models created using Autodesk Inventor 2014. The uppermost portions of the branches were not modeled because they are very thin (less than 10 mm in diameters).

2.3. Simulation of the sample

ANSYS software (ANSYS 15.0, ANSYS, Inc., Canonsburg, USA) was used for simulation of the tree under loading conditions. To reduce the complexity of the tree system, the following hypotheses were made while simulating the tree motion:

- The trunks and branches were linear elastic isotropic material with different mechanical properties, including density and elastic modulus.
- All vibration energy from the shaker was transferred to trees.

The geometries were imported into ANSYS from Autodesk Inventor 2014 and meshed using solid 185 type elements. Transient dynamic analysis was used to simulate the tree motion, and the simulation was performed for 2 s. The input forces in the simulation were consistent with the experiment forces measured by a tension sensor (H3-C3-150KG, Zhonghang Electronic Measuring Instruments Co., Ltd, Xian, China) in the field experiment, as shown in Table 1.

2.4. Field experiments

The vibration experiments were conducted on three trees in the same field conditions. A hand-held electric shaker was used to apply vibratory excitations to the trees at the excitation points shown in Table 2.

The shaker was adapted from a battery powered reciprocating saw (Metabo Power tools (China) Co., Ltd, Shanghai, China) by replacing the saw blade with a shaker head and adding a frequency controller. The shaker could provide a stroke of 18 mm and vibration frequency up to 50 Hz. The vibration frequency was controlled using a frequency controller. Magnitude of vibration force was measured using the tension sensor (H3-C3-150KG, Zhonghang Electronic Measuring Instruments Co., Ltd, Xian, China) mounted in the shaker head, as shown in Fig. 3(e). The shaker head acted on the trunk as an impact excitation. Acceleration transducers (DH311E, Donghua Testing Technology Co., Ltd, Taizhou, China) were used to measure the dynamic responses of branches recorded by a data collector (DH5922, Donghua Testing Technology Co., Ltd, Taizhou, China), as shown in

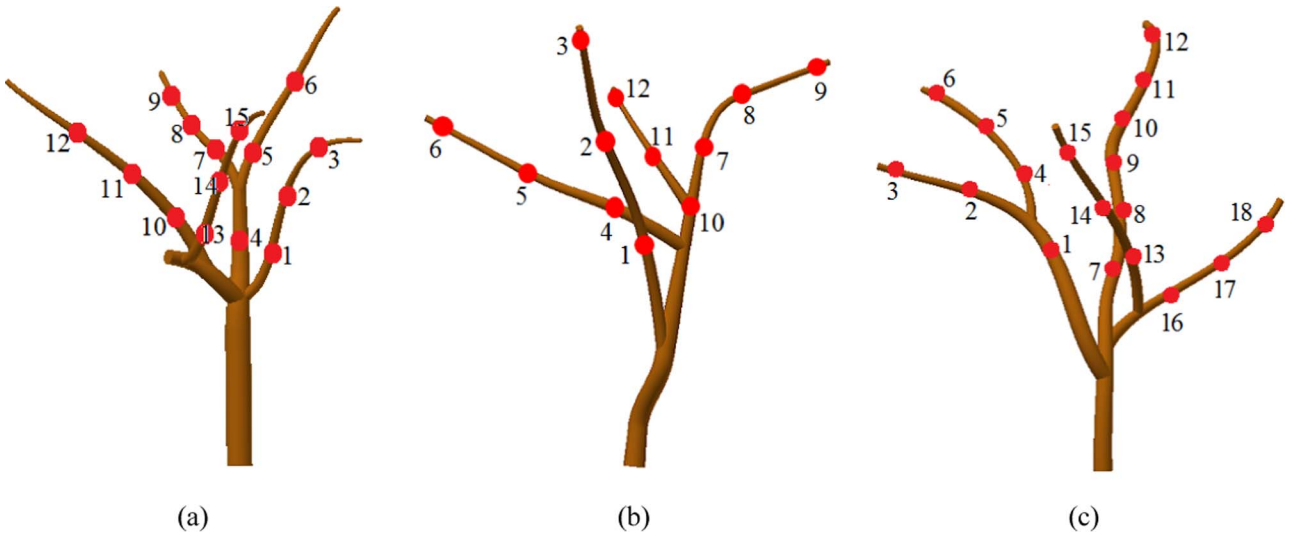

Fig. 2. Three jujube tree models created in Autodesk Inventor 2014, and selected points marked by red dot. (a) Tree 1, (b) Tree 2, (c) Tree 3.

Table 1
Magnitude and frequency of input force in the simulation and field experiments.

Frequency (Hz)	5.0	10.0	15.0	20.0	25.0
Force (N)	121.8	242.5	263.0	288.1	367.2

Table 2
Geometric dimensions and excitation positions of the trees.

No.	Age/years	Diameter of trunk/m	Height/m	Position of excitation/m
Tree 1	6	0.086	1.35	0.35
Tree 2	6	0.069	1.26	0.35
Tree 3	6	0.054	1.23	0.35

Note: Positions of excitation are characterized by the distance between excitation point and root.

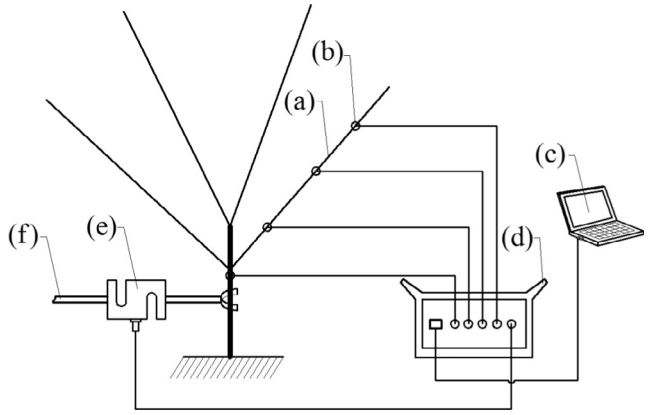

Fig. 3. Schematic of experimental setup and data acquisition. (a) Branches, (b) acceleration meter, (c) computer, (d) data collector, (e) tension sensor, and (f) shaker head.

Fig. 3(b) and (d).

The main test procedures were as followed: first, mount the transducers on the measured locations of branches. Measured locations were set 0.2 m apart on each branch starting from branches crotch, and the distance between each monitoring point along the branches is 0.2 m, as shown in Fig. 2. Second, turn on the data collector and recording software, and then, the shaker started to act on the trunk to ensure that vibration data were collected. The vibration frequencies had five groups including 5, 10, 15, 20, and 25 Hz. The vibration time of each excitation was 2 s. Next, uninstalled the transducers and mounted them on another branch. Follow such steps until the entire tree was tested.

The accelerations of different branches were measured separately because of limited acceleration transducers and data recording channels. Each four points were recorded once. In order to reduce the error, we insured that the input force had same magnitude and frequency.

3. Results and discussion

3.1. Mechanical properties of jujube tree

The properties of different parts in the trees are shown in Table 3. These values show a variability of mechanical characteristics between the trunk and branch. The density, moisture, and Poisson ratio of the branch are larger than that of the trunk, while the Young's modulus and shear modulus of the branch are smaller than that of the trunk.

To our knowledge, very few work on the mechanical characteristics of jujube tree wood are published. In the harvesting season, the moisture of branch is higher than that of trunk, which results of the larger density of branch than the trunk (Yang et al., 2012). This could be explained by girdling on the trunk near the root of jujube trees, which made the moisture and nutrition stay in the upper part of tree

Table 3
Summary of properties measured and calculated.

Property	Measured or calculated value	Standard deviation
Density of branch (kg/m^3)	1013.89	86.87
Density of trunk (kg/m^3)	931.46	60.61
Moisture of branch (%)	39.2	7.90
Moisture of trunk (%)	32.24	2.15
Young's modulus of branch (MPa)	1208.43	250.32
Young's modulus of trunk (MPa)	2188.43	145.85
Shear modulus of branch (MPa)	437.84	90.69
Shear modulus of trunk (MPa)	770.57	51.36
Poisson ratio of branch (no unit)	0.42	–
Poisson ratio of trunk (no unit)	0.38	–
Damping ratio (no unit)	0.04	–

(Jia et al., 2015).

3.2. Acceleration of simulation and experiment

Acceleration at different points along the trees branches were measured using the simulation and experimental methods. The average and maximum resultant acceleration values at each select point were monitored at the five shaking frequencies (5, 10, 15, 20, and 25 Hz), and the results are reported in Fig. 4.

It can be seen from Fig. 4 that the accelerations from field experiments were generally greater than that from simulation. The figures also show that the acceleration of most points at the top of branches are at the peak of experimental and simulation curves. Both experimental and simulation curves reveal that acceleration of points increased from the bottom to top of branches.

By comparing the accelerations at the five frequencies, it can be observed that the acceleration increased with the increase of shaking frequency. Generally, the acceleration curve for most points have similar changing trends excluding some individual points, such as point 13, 14 and 15 in Tree 1. The reason is that the branches where these points located were very thin, and a relatively large energy loss between the acceleration transducer and the branch which may be caused by the damping activities of branches and the small contact area between transducers and branches.

The maximum resultant acceleration of the experiment and simulation were also shown in Fig. 4. The experimental value of the maximum resultant acceleration is larger than the simulation value. However, the curves changing trends showed a poor alignment. Only several points have similar trends. The main reason is that the direction of input force in the simulation model is not completely consistent with that in the experiment. In the simulation model the force is in the direction of the coordinate axis. However, during the experiment, it might have been the direction of force is not in line with the coordinate axis.

Because of the differences in the trees and the difference of the locations from their respective local origins, the ratio of resultant acceleration values between experiment and simulation is calculated to study all the three trees, as shown in Table 4. It can be observed that both the average and maximum resultant acceleration values were higher in the experimental values since all the mean larger than 1 in Table 4. The mean of average acceleration ratios were from 0.96 (25 Hz of Tree 1) to 3.45 (10 Hz of Tree 2), and most standard deviations were less than 1.0. The standard deviation (std) of maximum acceleration ratio were larger than that of average acceleration ratio. It indicated that the experimental values and simulation values of average resultant accelerations have similar changing tendency.

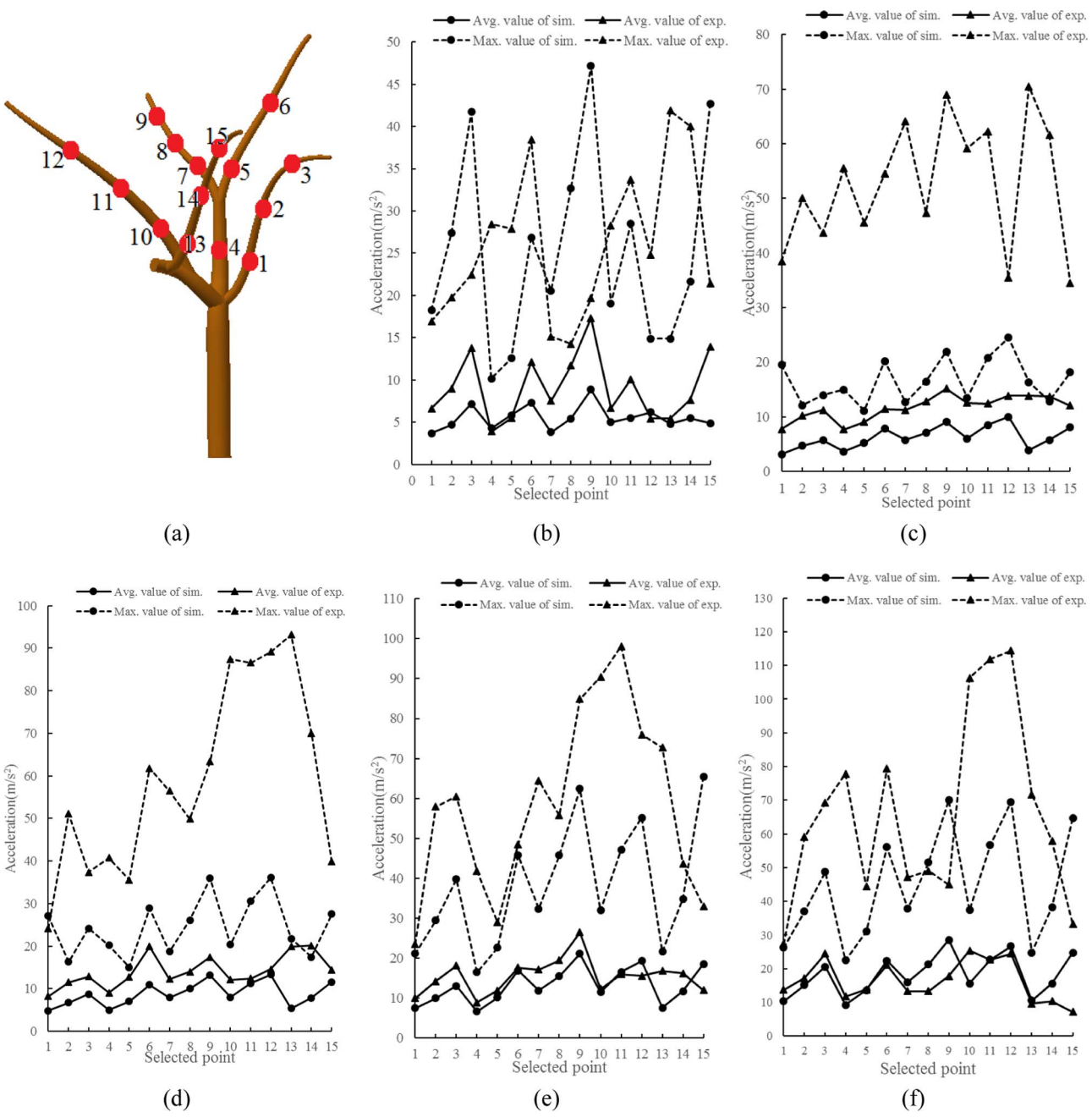

Fig. 4. Fifteen selected points of Tree 1 for analysis marked by red dot (a), and resultant accelerations of the 15 selected points at the five frequencies of (b) 5 Hz, (c) 10 Hz, (d) 15 Hz, (e) 20 Hz, and (f) 25 Hz.

Therefore, the acceleration value of each part of a tree under the vibration can be predicted using the average simulation values. The inertia force value of the point can be calculated by the acceleration value. Consequently, when evaluating the fruit removal efficiency or vibration energy transmission loss, the simulation method is possible to be a choice instead of the complex and time-consuming field experiment.

3.3. Correlation analysis

To investigate the reasons why the acceleration curves changing trends were similar, correlation coefficients between experimental and simulation values were analyzed, as shown in Table 5. It indicated that the experimental and simulation values of average resultant acceleration showed a good correlation. All the correlation coefficients of average resultant accelerations are larger than 0.5, and the largest value of 0.80 was obtained at the 5 Hz of Tree 3. The results of ANOVA analysis (Table 5) also indicate that there are no significant differences between any two trees' resultant acceleration correlation coefficients. The mean coefficient of the three trees is 0.62, which is larger than the mean correlation coefficient of 0.58 obtained by Savary et al. (2010) for citrus trees.

The correlation of the maximum resultant accelerations between the experiment and simulation is relatively lower than that of the average resultant accelerations. Furthermore, some correlation coefficients are negative, and the mean absolute value of coefficients is 0.28. In general, the maximum resultant accelerations of experiment and simulation showed a poor correlation.

A perfect correlation between the simulation and experimental resultant acceleration values was not expected. This is because of the

Table 4
Ratio of resultant acceleration values between experiment and simulation of the three trees at the five different frequencies.

Point	Average acceleration ratio (experimental value/simulation value)															Maximum acceleration ratio (experimental value/simulation value)													
	Tree 1					Tree 2					Tree 3					Tree 1					Tree 2					Tree 3				
	5	10	15	20	25	5	10	15	20	25	5	10	15	20	25	5	10	15	20	25	5	10	15	20	25	5	10	15	20	25
1	1.79	2.44	1.71	1.34	1.33	1.15	2.53	2.55	2.56	1.31	0.94	2.75	2.78	1.99	1.44	0.93	1.97	0.89	1.11	1.04	2.41	2.54	2.78	1.72	1.42	1.71	5.92	3.53	3.50	1.67
2	1.91	2.16	1.72	1.42	1.14	1.36	1.41	1.44	2.57	1.06	0.80	3.05	2.97	1.96	1.48	0.72	4.13	3.13	1.96	1.59	2.09	1.67	4.50	1.27	1.57	1.36	7.38	5.18	3.85	1.17
3	1.92	1.96	1.48	1.38	1.19	1.92	3.79	2.32	3.00	1.95	2.31	3.54	3.31	2.23	0.64	0.54	3.12	1.54	1.52	1.42	3.65	7.66	10.08	2.09	3.24	5.44	7.97	6.09	6.56	3.72
4	0.91	2.11	1.80	1.34	1.27	1.37	2.14	1.68	2.43	0.78	2.17	1.45	2.89	2.94	0.95	2.80	3.71	2.01	2.54	3.46	2.46	1.58	1.65	2.77	1.29	2.16	1.38	4.03	9.26	2.09
5	0.94	1.73	1.81	1.17	1.01	1.28	3.03	2.03	2.64	1.12	2.25	1.75	3.97	2.56	0.56	2.22	4.08	2.37	1.28	1.43	2.06	2.91	2.97	4.01	2.47	3.26	1.70	5.81	14.27	4.75
6	1.65	1.46	1.83	1.05	0.94	2.55	2.17	2.03	1.65	1.26	2.58	1.27	2.44	2.96	0.94	1.43	2.69	2.14	1.06	1.42	7.06	2.81	5.08	4.15	2.53	4.20	1.82	4.43	10.18	2.17
7	1.97	1.95	1.55	1.44	0.83	2.16	2.84	1.69	2.17	1.06	0.95	1.03	1.32	1.41	1.27	0.74	5.05	3.02	1.99	1.25	1.78	3.72	1.51	2.81	0.57	1.61	1.22	1.26	1.32	2.46
8	2.15	1.81	1.40	1.25	0.63	1.96	2.17	2.06	2.64	0.99	0.90	1.34	1.61	1.28	1.07	0.44	2.88	1.91	1.22	0.95	2.54	3.21	4.24	4.55	1.51	1.73	2.26	2.26	2.01	2.43
9	1.96	1.67	1.33	1.25	0.62	2.74	4.75	2.78	4.37	1.39	0.69	1.02	1.74	1.25	1.17	0.42	3.15	1.76	1.36	0.64	5.23	9.79	10.53	9.44	2.94	0.79	1.27	1.61	1.93	2.68
10	1.33	2.09	1.53	1.07	1.62	1.10	3.85	2.30	2.92	1.10	1.27	1.23	2.02	1.35	1.37	1.48	4.38	4.29	2.83	2.85	2.38	6.04	3.65	4.21	1.57	2.64	2.65	1.04	2.80	1.05
11	1.83	1.46	1.10	0.97	1.00	2.02	6.41	3.20	2.29	1.34	0.84	1.89	1.86	1.83	1.39	1.18	2.99	2.83	2.08	1.97	1.92	16.79	5.98	6.40	4.22	1.07	4.15	2.14	4.82	2.37
12	0.88	1.38	1.10	0.81	0.92	1.84	6.32	3.67	3.42	2.53	1.21	2.12	2.03	1.28	1.44	1.66	1.45	2.47	1.38	1.64	2.80	19.53	10.12	13.26	7.36	3.30	5.59	2.60	2.86	1.97
13	1.14	3.55	3.72	2.23	0.92	–	–	–	–	–	1.09	1.82	3.97	1.23	1.52	2.81	4.30	4.28	3.37	2.90	–	–	–	–	–	1.02	2.21	5.71	2.45	0.89
14	1.39	2.38	2.57	1.39	0.66	–	–	–	–	–	1.20	1.24	2.67	1.49	1.40	1.85	4.79	4.01	1.25	1.51	–	–	–	–	–	2.16	1.66	4.07	3.65	1.15
15	2.86	1.49	1.25	0.64	0.29	–	–	–	–	–	1.23	1.31	3.47	1.07	1.17	0.50	1.90	1.45	0.50	0.51	–	–	–	–	–	2.88	2.70	4.36	2.61	1.89
16	–	–	–	–	–	–	–	–	–	–	1.72	1.78	3.91	1.74	1.16	–	–	–	–	–	–	–	–	–	–	2.83	1.65	6.88	5.85	2.21
17	–	–	–	–	–	–	–	–	–	–	1.28	1.09	2.76	2.35	0.89	–	–	–	–	–	–	–	–	–	–	0.89	2.23	11.58	6.02	3.57
18	–	–	–	–	–	–	–	–	–	–	2.21	2.14	3.06	2.27	0.76	–	–	–	–	–	–	–	–	–	–	4.04	4.67	25.31	7.99	3.17
Mean	1.64	1.98	1.73	1.25	0.96	1.79	3.45	2.31	2.72	1.32	1.42	1.77	2.71	1.84	1.15	1.31	3.37	2.54	1.70	1.64	3.03	6.52	5.26	4.72	2.56	2.39	3.25	5.44	5.11	2.30
Std	0.55	0.55	0.66	0.36	0.33	0.54	1.64	0.65	0.68	0.48	0.61	0.72	0.83	0.60	0.30	0.82	1.09	1.05	0.76	0.84	1.58	6.00	3.27	3.50	1.82	1.29	2.16	5.56	3.45	1.01

Table 5
Correlation coefficients between the experiment and simulation for average and maximum acceleration.

Frequency	Average resultant acceleration			Maximum resultant acceleration		
	Tree 1	Tree 2	Tree 3	Tree 1	Tree 2	Tree 3
5	0.67	0.77	0.80	−0.34	0.43	0.40
10	0.66	0.57	0.60	−0.16	−0.31	0.17
15	0.68	0.55	0.62	0.25	−0.36	−0.29
20	0.62	0.51	0.50	0.31	−0.16	−0.22
25	0.58	0.55	0.73	0.19	−0.14	0.20
Mean ± Std	0.64 ± 0.04[a]	0.59 ± 0.10[a]	0.62 ± 0.11[a]	0.05 ± 0.28[A]	−0.11 ± 0.32[A]	0.05 ± 0.29[A]

Note: The same lower-case letters are not significantly different at 0.05 level from each average acceleration, and the same capital letters are not significantly different at 0.05 level from each maximum acceleration.

differences between the actual system and the model developed to describe the system, such as small branches were not modeled that affects the damping of the entire tree structure and the method used for measurement of the coordinates on the tree structure was not very accurate. Therefore, the simulation might be improved by dividing the tree into more parts, and using anisotropic properties materials for wood, and establishing a more accurate 3D model for tree.

3.4. Resultant acceleration distribution

Generally, the inertia force of the fruit is an index to judge whether the force is sufficient to detach the fruit or not. The magnitude of acceleration determines the inertia force according to Newton's first law. The acceleration distribution can be used to evaluate the parts where fruits detachment is more probable. In the simulation, the distribution nephogram was also analyzed to know the regions with increased acceleration. Fig. 5 showed the resultant acceleration distribution of Tree 1 result from simulation. From Fig. 5, it is obviously that the resultant acceleration increases with the increase of shaking frequency. From the resultant acceleration distribution, it also can be observed that the acceleration increases gradually from the crotch to the top of branch, which is in accordance with the results of Fig. 4.

In order to validate the results from the distribution nephogram, the selected points of the three trees were divided into two groups. The threshold for dividing is the midpoint of each branch. One group is the points at the bottom of a branch, named as “bottom group (BG)”, and the other is the remaining points of a branch, named as “top group (TG)”. The mean of average resultant accelerations of the selected points in the two groups (BG and TG) of each tree were calculated and TG/BG ratios of each tree at different frequencies were employed because of the differences in the trees and branches and frequencies, as shown in Table 6. From Table 6, it is indicated that the acceleration of

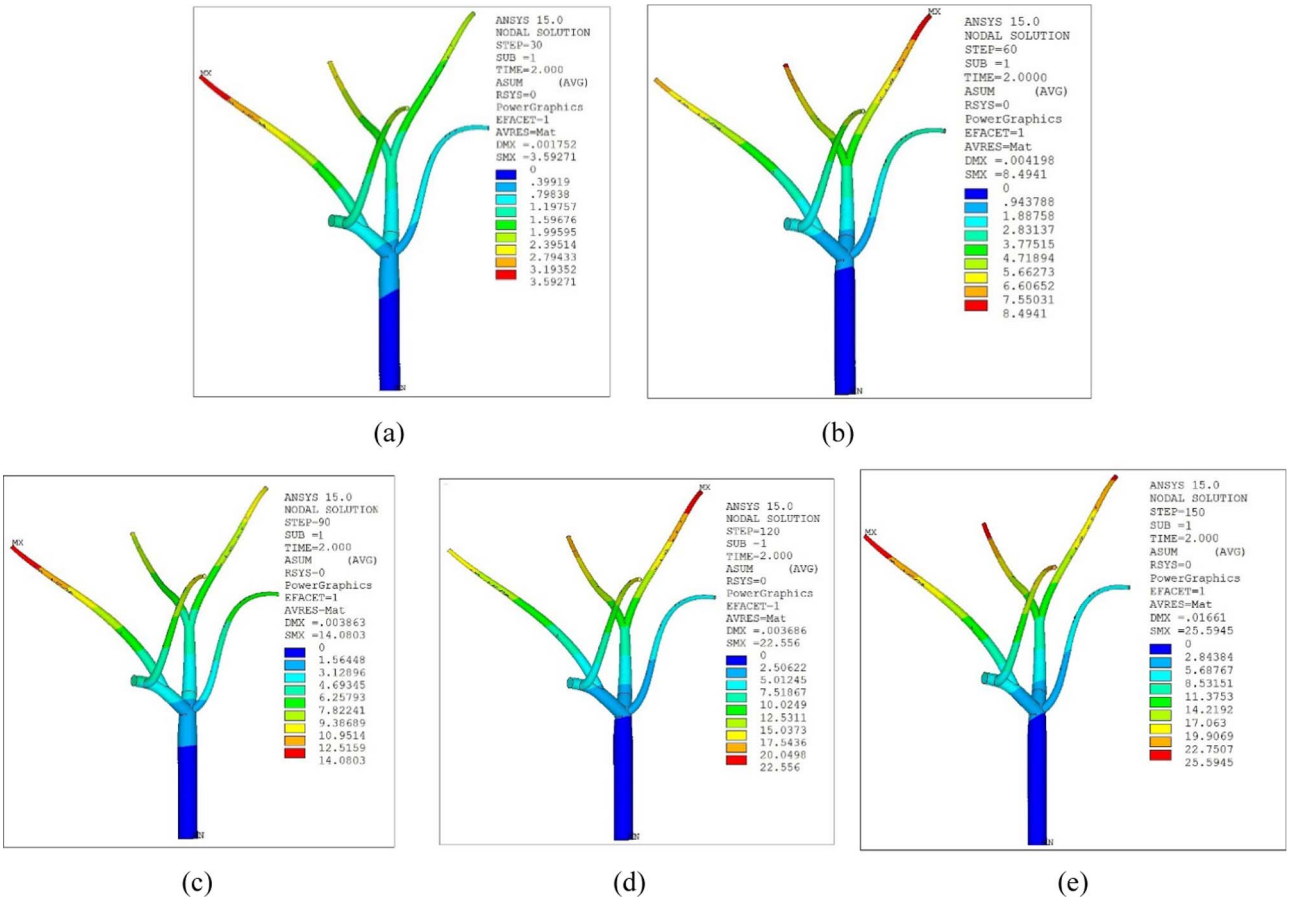

Fig. 5. Average resultant acceleration distribution nephogram at the end of simulation of Tree 1 at the five different frequencies. (a) 5 Hz, (b) 10 Hz, (c) 15 Hz, (d) 20 Hz, and (e) 25 Hz.

Table 6
Mean of average resultant accelerations of the selected points in the two groups of "bottom group (BG)" and the "top group (TG)" and their ratios of TG/BG at the five different frequencies of each tree.

Frequency	Tree1			Tree2			Tree3		
	BG	TG	TG/BG	BG	TG	TG/BG	BG	TG	TG/BG
5	5.94	11.03	1.86	15.99	25.89	1.62	21.27	24.37	1.15
10	4.64	8.09	1.75	45.85	99.47	2.17	43.56	87.26	2.00
15	8.01	11.20	1.40	56.17	83.38	1.48	70.71	143.92	2.04
20	9.18	17.11	1.86	80.25	113.82	1.42	120.72	182.98	1.52
25	12.59	23.26	1.85	45.82	88.72	1.94	53.95	110.01	2.04
Mean ± Std	–	–	1.74 ± 0.20[a]	–	–	1.73 ± 0.32[a]	–	–	1.75 ± 0.40[a]

Note: The same letters are not significantly different at 0.05 level from each ratio of TG to BG.

the selected points in TG are significantly greater than that in the BG, which is coincident the observation from the distribution nephogram. All the ratios of TG/BG are larger than 1.0, and there are no significant differences among the three trees. These results indicated that the points in the top of branch have larger accelerations, which suggest that fruits in those area are more easier to be harvested (Zhou, 2014). This observation can be as a guide for fruit tree pruning and mechanical vibration harvesting.

4. Conclusion

Chinese winter jujube trees were modeled using Autodesk Inventor 2014 and then simulated for vibration harvesting by finite element method in ANSYS 15.0 based on some assumptions. In simulation, the tree model was divided to two parts, including branches and trunk. For both parts, the wood's mechanical properties were determined experimentally. Field experiments were conducted using a shaker at five frequencies (5, 10, 15, 20, and 25 Hz) on three trees.

It was observed that the acceleration value of experiment is generally larger than that of simulation, and it increases from the bottom of branch to the top. The acceleration curves in both experimental and simulation conditions and the distribution nephograms indicated that the greater frequency of tree shaking generates greater acceleration. The average resultant accelerations from the simulation is promising for evaluating the actual vibration harvesting since they have similar changing trends, instead of the complex and time-consuming field experiment.

The simulation results can be further improved by using the anisotropic properties of trunk and branch and developing a more extensive model of the trees. From this study, it can be concluded that the simulation framework used here can be applied for studying the response of trees under the vibration excitation of the shaker. This framework can be utilized for improvements in shaker design to improve harvesting efficiency and energy distribution.

Acknowledgements

The work was supported by the Key Research and Development Program in Shaanxi Province of China (Project No. 2017NY-164), and the National Natural Science Foundation of China (Grant No. 31301242), and the China Postdoctoral Science Foundation (Grant No. 2015M572602), and the International Scientific and Technological Cooperation Foundation of Northwest A & F University (A213021505). The authors would like to express our great thanks Dr. Jianfeng Zhou from University of Missouri and Dr. Ahmad Al-Mallahi from the FUJI Project of Bosch Corporation in Japan for their advice and support to the manuscript writing and English editing.

References

Bentaher, H., Haddar, M., Fakhfakh, T., Mâalej, A., 2013. Finite elements modeling of olive tree mechanical harvesting using different shakers. Trees 27, 1537–1545. http://dx.doi.org/10.1007/s00468-013-0902-0.

Du, X., Chen, D., Zhang, Q., Scharf, P.A., Whiting, M.D., 2012. Dynamic responses of sweet cherry trees under vibratory excitations. Biosys. Eng. 111, 305–314. http://dx.doi.org/10.1016/j.biosystemseng.2011.12.009.

Fu, L., Peng, J., Nan, Q., He, D., Yang, Y., Cui, Y., 2016. Simulation of vibration harvesting mechanism for sea buckthorn. Eng. Agri. Environ. Food 9, 101–108. http://dx.doi.org/10.1016/j.eaef.2015.08.003.

Fu, W., He, R., Qu, J., Wang, L., Ka, Z., 2014. Design of self-propelled dwarf and close planting jujube harvester. J. Agric. Mech. Res. 36, 106–109. http://dx.doi.org/10.3969/j.issn.1003-188X.2014.04.026.

Gao, Q., Wu, C., Wang, M., 2013. The jujube (*Ziziphus jujuba* Mill.) fruit: a review of current knowledge of fruit composition and health benefits. J. Agric. Food Chem. 61, 3351–3363. http://dx.doi.org/10.1021/jf4007032.

Gao, Q., Wu, P., Liu, J., Wu, C., Parry, J.W., Wang, M., 2011. Physico-chemical properties and antioxidant capacity of different jujube (*Ziziphus jujuba* Mill.) cultivars grown in loess plateau of China. Sci. Hortic. 130, 67–72. http://dx.doi.org/10.1016/j.scienta.2011.06.005.

Jia, X., Cao, L., Wen, Z., Liu, X., 2015. Effect of girdling on the organic nutrition of sheding shoots of ziziphus jujube cv. dongzao. North. Hortic. 32–44. http://dx.doi.org/10.11937/bfyy.201522007.

Jing, X., Lang, Z., 2009. Frequency domain analysis of a dimensionless cubic nonlinear damping system subject to harmonic input. Nonlinear Dyn. 58, 469–485. http://dx.doi.org/10.1007/s11071-009-9493-0.

Krauss, A., 2007. Some new aspects of calculation of wood adsorptive stress. Wood Res. 52, 23–34.

Láng, Z., 2008. A one degree of freedom damped fruit tree model. Trans. ASABE 51, 823–829. http://dx.doi.org/10.13031/2013.24520.

Lam, C.T.W., Chan, P.H., Lee, P.S.C., Lau, K.M., Kong, A.Y.Y., Gong, A.G.W., Xu, M.L., Lam, K.Y.C., Dong, T.T.X., Lin, H., Tsim, K.W.K., 2016. Chemical and biological assessment of Jujube (*Ziziphus jujuba*)-containing herbal decoctions: Induction of erythropoietin expression in cultures. J. Chromatogr. 1026, 254–262. http://dx.doi.org/10.1016/j.jchromb.2015.09.021.

Lee, S., Huh, Y., So, J., Min, K., Kim, G., 2003. Mechanical Jujube (*Zizyphus Jujuba* Miller) Harvester. CSAE/SCGR Meeting Montreal, Quebec.

Li, J., Fan, L., Ding, S., Ding, X., 2007. Nutritional composition of five cultivars of Chinese jujube. Food Chem. 103, 454–460. http://dx.doi.org/10.1016/j.foodchem.2006.08.016.

Meng, X., Tang, Z., Shen, C., Jia, S., Liu, W., Zhou, Y., Zheng, X., 2013. 4YS-24 type jujube harvester. Xinjiang Agric. Mech. 29, 13–14. http://dx.doi.org/10.3969/j.issn.1007-7782.2010.01.014.

Plastina, P., Bonofiglio, D., Vizza, D., Fazio, A., Rovito, D., Giordano, C., Barone, I., Catalano, S., Gabriele, B., 2012. Identification of bioactive constituents of Ziziphus jujube fruit extracts exerting antiproliferative and apoptotic effects in human breast cancer cells. J. Ethnopharmacol. 140, 325–332. http://dx.doi.org/10.1016/j.jep.2012.01.022.

Razavi, S.M.A., BahramParvar, M., 2007. Some physical and mechanical properties of kiwifruit. Int. J. Food Eng. 3, 1–14. http://dx.doi.org/10.2202/1556-3758.1276.

Savary, S.K.J.U., Ehsani, R., Salyani, M., Hebel, M.A., Bora, G.C., 2011. Study of force distribution in the citrus tree canopy during harvest using a continuous canopy shaker. Comput. Electron. Agric. 76, 51–58. http://dx.doi.org/10.2202/1556-3758.1276.

Savary, S.K.J.U., Ehsani, R., Schueller, J.K., Rajaraman, B.P., 2010. Simulation study of citrus tree canopy motion. Trans. ASABE 53, 1373–1381. http://dx.doi.org/10.13031/2013.34892.

Stoffler, G., 1980. Determination of torsion strength and shear moduli of a multi-layer composite. J. Compos. Mater. 14, 95–110. http://dx.doi.org/10.1016/0010-4361(81)90438-9.

Sun, L., Liu, M., Zhu, S., Jie, Z., Wang, M., 2007. Effect of nitric oxide on alcoholic fermentation and qualities of Chinese winter jujube during storage. Agric. Sci. China 6, 849–856. http://dx.doi.org/10.1016/S1671-2927(07)60121-7.

Tang, X., Ren, J., Liu, C., Xiao, D., 2011. Simulation of Vibration Harvesting Mechanism for Wolfberry. In: ASABE Annual International Meeting, Louisville Kentucky USA.

Tinoco, H.A., Ocampo, D.A., Peña, F.M., Sanz-Uribe, J.R., 2014. Finite element modal analysis of the fruit-peduncle of *Coffea arabica* L. var. Colombia estimating its geometrical and mechanical properties. Comput. Electron. Agric. 108, 17–27. http://dx.doi.org/10.1016/j.compag.2014.06.011.

Upadhyaya, S.K., Cooke, J.R., Rand, R.H., 1981. Limb impact harvesting, part I: finite element analysis. Trans. ASABE 24, 856–863. http://dx.doi.org/10.13031/2013.34352.

Wu, C., He, L., Du, X., Chen, S., Ni, K., 2014. 3D reconstruction of Chinese hickory tree for dynamics analysis. Biosys. Eng. 119, 69–79. http://dx.doi.org/10.1016/j.biosystemseng.2014.01.008.

Yang, Y., Lu, G., Liu, H., 2012. Research on water content in foliages of ziziphus jujuba. Shanxi For. Sci. Tech. 41, 1–5. http://dx.doi.org/10.3969/j.issn.1007-726X.2012.01.002.

Yung, C., Fridley, R., 1975. Simulation of vibration of whole tree systems using finite elements Trans. ASAE 3, 475–481. http://dx.doi.org/10.13031/2013.36613.

Zhang, L., Li, S., Dong, Y., Zhi, H., Zong, W., 2016. Tea polyphenols incorporated into alginate-based edible coating for quality maintenance of Chinese winter jujube under ambient temperature. LWT - Food Sci. Technol. 70, 155–161. http://dx.doi.org/10.1016/j.lwt.2016.02.046.

Zhou, J., He, L., Zhang, Q., Du, X., Chen, D., Karkee, M., 2013. Evaluation of the influence of shaking frequency and duration in mechanical harvesting of sweet cherry. Appl. Eng. Agric. 29, 607–612. http://dx.doi.org/10.13031/aea.29.9917.

Zhou, J., 2014. Vibratory Harvesting Technology Research for Fresh Market Sweet Cherry. [Doctor of Philosophy]. Washington State University.